Glyoxal cross-linking of solubilised extracellular matrix to produce highly porous, elastic and chondro-permissive scaffolds for orthopaedic tissue engineering

David C. Browe [1 2 3], Olwyn R. Mahon[1 4], Pedro J. Díaz-Payno [1 2 3] Nina Cassidy[1], Ivan Dudurych[1], Aisling Dunne [4], Conor T. Buckley [1 2 3], Daniel J. Kelly*[1 2 3]

*Corresponding Author: Tel: +353-1-8963947, email: kellyd9@tcd.ie

[1] Trinity Centre for Bioengineering, Trinity Biomedical Sciences Institute, Trinity College Dublin, Ireland.

[2] Department of Mechanical and Manufacturing Engineering, School of Engineering, Trinity College Dublin, Ireland.

[3] Advanced Materials and Bioengineering Research Centre (AMBER), Royal College of Surgeons in Ireland and Trinity College Dublin, Ireland.

[4] School of Biochemistry and Immunology and School of Medicine, Trinity Biomedical Sciences Institute, Trinity College Dublin, Ireland.

ABSTRACT

Extracellular matrix (ECM) derived implants hold great promise for tissue repair, but new strategies are required to produce efficiently decellularized scaffolds with the necessary porosity and mechanical properties to facilitate regeneration. In this study we demonstrate that it is possible to produce highly porous, elastic, articular cartilage ECM derived scaffolds that are efficiently decellularized, nonimmunogenic and chondro-permissive. Pepsin solubilised porcine articular cartilage was cross-linked with glyoxal, lyophilized and then subjected to dehydrothermal treatment. The resulting scaffolds were predominantly collagenous in nature, with the majority of sGAG and DNA removed during scaffold fabrication. Four scaffold variants were produced to examine the effect of both ECM (10 or 20 mg/ml) and glyoxal (5mM or 10mM) concentration on the mechanical and biological properties of the resulting construct.. When seeded with human infrapatellar fat pad derived stromal cells (FPSCs), the scaffolds with the lowest concentration of both ECM and glyoxal were found to promote the development of a more hyaline-like cartilage tissue, as evident by increased sGAG and type II collagen deposition. Furthermore, when cultured in the presence of human macrophages, it was found that these ECM derived scaffolds did not induce the production of key pro-inflammatory cytokines, which is critical to success of an implantable biomaterial. Together these findings demonstrate that the novel combination of solubilised articular cartilage ECM and glyoxal crosslinking can be used to produce highly porous scaffolds that are sufficiently decellularized, highly elastic, chondro-permissive and do not illicit a detrimental immune response when cultured in the presence of human macrophages.

Keywords: Extracellular matrix, Cartilage, Scaffold, Decellularization, Tissue engineering, Immune response.

1. Introduction

Due in part to its lack of vasculature, articular cartilage possesses a relatively poor intrinsic capacity for repair and as such external factors such as cells, growth factors, biomaterials or a combination of these must be delivered to the site of injury to promote repair of damaged joints [1-3]. Current clinical treatment options for articular cartilage repair such as micro-fracture remain sub-optimal, with the repair tissue generally consisting of bio-mechanically inferior fibro-cartilage [4]. Xenogeneic extracellular matrix (ECM) derived biological scaffolds have been used in a variety of clinical indications, promoting tissue repair by providing both structural and functional cues to resident cells [5,6]. ECM scaffolds fabricated from decellularized animal or human articular cartilage tissue are promising biomaterials for articular cartilage regeneration due to their inherent chondro-inductivity [7-19]. Such biological scaffolds typically take one of two forms. Particulated or solubilised cartilage ECM can be freeze dried and subsequently cross-linked, resulting in porous scaffolds with relatively poor mechanical properties when compared to native articular cartilage [20-22]. Alternatively, intact cartilage explants can be decellularized without disrupting the overall collagen network, resulting in a graft with more desirable mechanical properties but with a porosity that limits cellular infiltration [23-25]

The success or failure of any implantable biomaterial is also invariably linked to the host immune response. The host innate and adaptive immune system can respond to cellular antigens and DNA within ECM derived constructs, or various components of the ECM itself. Ineffectively decellularized ECM scaffolds retain remnants of cellular material which can elicit proinflammatory cytokine production and adverse tissue remodelling [26-28]. One of the key criteria set as confirmation of successful decellularization is to obtain a DNA content of less than 50ng per mg of dry weight [29]. However, overly harsh decellularization protocols can have a detrimental impact on the bioactivity and biomechanical properties of the resulting biomaterial. Protocols that employ the use of detergents such as Sodium Dodecyl Sulfate (SDS)

can dramatically reduce the proteoglycan content of the tissue, negatively impacting the mechanical properties of the resulting grafts. Furthermore, freeze-thaw cycles that are commonly employed in decellularization protocols can result in disorder of the collagen network due to ice crystal formation [6,30].

In the case of scaffolds generated by freeze-drying particulated or solubilized ECM, physical and chemical crosslinking methodologies are generally applied in order to maintain the structural integrity and porosity of the resulting scaffold architecture [31,32]. However, the use of chemical crosslinkers can have a detrimental effect due to the cytotoxicity of the reagents used. Glutaraldehyde is a commonly used chemical crosslinker for collagen based biomaterials, however cytotoxicity can become an issue at higher concentrations [33,34]. Biomaterials which have been cross-linked with glutaraldehyde can also induce a strong humoral immune response *in vivo* [35]. In addition, chemical crosslinking can also attenuate ECM scaffold degradation *in vivo* and as such negatively alter the host response to the implanted biomaterial [36]. Therefore, the degree and method of crosslinking *are* vital parameters to consider when using ECM-derived scaffolds for tissue repair applications.

This study examines the use of glyoxal as a chemical crosslinker, in addition to physical crosslinking using dehydrothermal (DHT) treatment, to produce porous and highly elastic ECM derived scaffolds for musculoskeletal tissue engineering. The crosslinking chemistry of glyoxal is similar to that of glutaraldehyde but with a reduced cytotoxic profile [37]. By solubilizing articular cartilage ECM prior to cross-linking and freeze-drying, we hypothesize that it is possible to produce efficiently decellularized, yet mechanically competent, ECM derived scaffolds that are nonimmunogenic and capable of facilitating the differentiation of adult stem cells towards a hyaline cartilage phenotype. Our specific goals were to fabricate and ascertain the biochemical and physical characteristics of the resulting scaffolds and the extent of decellularization. To establish the optimal conditions for chondrogenic differentiation

of adult stem cells, we varied both the concentration of ECM in the scaffolds and the degree of chemical crosslinking. Finally, we examined the effect of the implant decellularization process on cytokine production by macrophages, key cellular regulators of tissue repair and inflammation.

2. Materials and Methods

2.1 Articular cartilage ECM solubilisation.

Articular cartilage (AC) was harvested, under sterile conditions, from the femoral condyle and trochlear ridge of 3-4 month old female pigs. The articular cartilage was shaved from the joint using a biopsy punch and subsequently diced into 1-2mm pieces using a scalpel. The cartilage pieces were pre-treated with 0.2M NaOH solution for 24 hours at 4°C with gentle agitation. Pre-treatment extracts the majority of sGAGs in the tissue as well as removing cellular components [38]. After removal of the pre-treatment solution the tissue was washed in sterile dH_2O. The cartilage was subsequently solubilised using a solution of 1500U/ml of pepsin (Sigma) in 0.5M acetic acid (Sigma) under rotation(4RPM) for 24 hours at room temperature. To remove insoluble material the tissue sample was centrifuged at 2500G for 1 hour. The supernatant containing the solubilised tissue was next transferred to a new tube and combined with a 5M NaCl (Sigma) solution to a final concentration of 0.9M NaCl in order to preferentially salt precipitate type II collagen from the sample [39]. The salt and collagen solution were mixed followed by equilibration overnight at 4°C and subsequently centrifuged at 2500G for 1 hour at 4°C. The supernatant was discarded, and the collagen pellet was resuspended in 0.5M acetic acid followed by rotation at 4RPM overnight at room temperature to fully solubilise the collagen. The salt precipitation procedure was then repeated a second time. The acid solubilised collagen was then transferred into a dialysis membrane (MWCO 6-8 kD

Spectrum Labs). Dialysis was performed against 0.02M Na_2HPO_4 for 48 hours at 4°C with agitation of the dialysate. The dialyzing solution was changed for fresh solution after 24 hours. Following dialysis, the solubilised AC solution was transferred to 24 well tissue culture plates (1ml/well) and lyophilized. Once lyophilized the solubilised AC was stored at -80°C prior to scaffold fabrication.

2.2 Scaffold fabrication

Four variants of AC-ECM scaffolds were fabricated, with two ECM concentrations and two cross-linker concentrations: 20mg/ml AC crosslinked with 10mM glyoxal (20mg/10mM), 20mg/ml AC crosslinked with 5mM glyoxal (20mg/5mM), 10mg/ml AC crosslinked with 10mM glyoxal (10mg/10mM) and 10mg/ml AC crosslinked with 5mM glyoxal (10mg/5mM). The concentrations of ECM and glyoxal were chosen based on preliminary optimization experiments (data not shown) which examined cell infiltration and glyoxal toxicity. Glyoxal was chosen as a cross-linker due to the fact that it results in relatively low levels of cytotoxicity when compared to other aldehyde cross-linkers such as glutaraldehyde [40]. In order to fabricate AC-ECM scaffolds, the lyophilized solubilised AC was first weighed using a balance and transferred to sterile tubes. Under sterile conditions, the lyophilized AC was resuspended in high glucose Dulbecco's Modified Eagle Medium (DMEM - Gibco) to yield a final concentration of 20mg/ml or 10mg/ml. The phenol red in the DMEM was used as an indicator of pH. To dissolve the AC, 80µl of 0.5M Acetic acid was added per ml of AC-ECM solution to yield a final concentration of 0.02M Acetic acid, the solution was pipetted several times to ensure homogeneous mixing. The AC solution was neutralised by adding 20µl volumes of 0.1M NaOH until the colour of the solution changed from yellow to red. The AC solution was then chemically crosslinked using glyoxal (Sigma) at a final concentration of 10mM or 5mM.

The solution was mixed well and incubated for 30 mins at 37°C to allow crosslinking to occur. After crosslinking the solution was transferred to custom made moulds (height 5mm and diameter 3mm) and freeze dried (FreeZone Triad, Labconco, KC, USA). To create porous scaffolds, the solution was initially frozen to -30°C at a rate of -1°C/min, this temperature was held for 1 hour before rising to -10°C at a rate of +1°C/min. Once at -10°C, this temperature was maintained under a vacuum of 0.2 mBar for 24 hours before the temperature was increased to +20°C at a rate of +1°C/min [9]. Scaffolds were physically crosslinked in a vacuum oven (VD23, Binder, Germany) by dehydrothermal (DHT) treatment at 115°C for 24 hours under vacuum (2 mBar).

To act as a positive control for immunological experiments, scaffolds were also fabricated from non-solubilised, particulated porcine articular cartilage as previously described [10]. Briefly, articular cartilage was harvested and then cyromilled (6770 Freezer/Mill, SPEX, UK) to a fine powder. This powder was then resuspended in dH_2O to create a 250mg/ml slurry. The slurry was then transferred into 5mm by 3mm moulds and was freeze-dried and DHT crosslinked using the same parameters as described above.

2.3 Scanning Electron Microscopy (SEM), pore size and porosity determination

Prior to SEM, scaffolds were sputter coated (108 auto sputter coater, Cressington, UK) with a gold/palladium alloy (Agar Scientific, UK) for 90 seconds at 0.1mBar. SEM images were obtained using a Zeiss Ultra Plus (Zeiss, Germany) with an acceleration voltage of 5kV and working distance of 5mm. To quantify the mean pore size of the various scaffolds, 5 images (containing a minimum of 100 pores) from 3 different scaffolds were measured using the analyse particle function of imageJ (National Institutes of Health Bethesda, Maryland) following thresholding of the images. Scaffold porosity was determined by gravimetry as

previously described [41,42]. Scaffolds were weighed using a digital mass balance and dimensions obtained using a vernier callipers in order to calculate density values.

2.4 Fat pad stromal cell (FPSC) isolation and expansion

Ethical approval for the donation of human infrapatellar fat pad (IFP) tissue and subsequent isolation of fat pad stromal cells (FPSCs) from the tissue was obtained from the institutional review board of the Mater Misericordae University Hospital Dublin. IFP tissue was obtained from three patients undergoing anterior cruciate ligament (ACL) reconstruction surgery. All three donors were male with a mean age of 28.6 years (26, 26 and 34 years old). FPSCs were isolated from IFP tissue as previously described [43-48]. Briefly, IFP tissue was washed with Phosphate Buffered Saline (PBS Sigma) followed by manual dicing with scalpels. IFP tissue was then incubated in high glucose DMEM (Gibco) containing 750U/ml collagenase II (Worthington Biochemical, NJ, USA) with Penicillin (100 U/ml) and streptomycin (100µg/ml) (both Gibco) for 3-4 hours until the tissue was fully digested. After digestion, insoluble tissue and residual fat was removed and discarded. The remaining cells were passed through cell strainers (Fisher Scientific), centrifuged and washed with D-PBS. Cells were then plated in T-175 flasks (Fisher Scientific) at a seeding density of $5x10^3$ cells/cm^2. FPSCs were expanded in DMEM supplemented with 10% FBS (Gibco), with Penicillin (100 U/ml) and streptomycin (100µg/ml) (both Gibco)and 5ng/ml fibroblast growth factor-2 (FGF-2, ProSpec-Tany, Israel) as previously described [49]. Expansion media was changed three times per week. FPSCs were not used beyond passage 3 for subsequent differentiation experiments.

2.5 Seeding AC-ECM scaffolds

Initially, to remove any residual DMEM all scaffolds were washed and rehydrated in D-PBS. To enhance seeding efficiency, the scaffolds were placed inside agarose moulds with a diameter of 5mm. The agarose moulds containing the scaffolds were then placed into 24-well

tissue culture plates (Fisher Scientific). To examine the ability of the various AC scaffolds to promote the chondrogenic differentiation of FPSCs *in vitro*, $0.5x10^6$ FPSCs were seeded onto individual scaffolds suspended in 25µl of expansion media. FPSCs were allowed to attach to the scaffolds for 1 hour in an incubator at 37°C. After FPSC attachment, 2.5ml of chemically defined chondrogenic differentiation media (CDM) was added per well. CDM consisted of high glucose DMEM supplemented with Penicillin (100 U/ml) and streptomycin (100µg/ml) (both Gibco*)*, 100µg/ml sodium pyruvate (Sigma), 40µg/ml L-Proline (Sigma), 50 µg/ml L-ascorbic acid-2-phosphate (Sigma), 1.5mg/ml bovine serum albumin (BSA-Sigma), 1X insulin transferrin selenium (ITS- Gibco), 100nM dexamethasone (Sigma) and 10ng/ml transforming growth factor beta-3 (TGF-β3 – ProSpec Tany, Israel). The FPSC seeded constructs were maintained in CDM for 28 days with the CDM being replenished three times per week.

2.6 Biochemical analysis of constructs

Cell free scaffolds (Day 0) and FPSC seeded constructs (Day 28) were analysed for DNA and sGAG content. Prior to performing assays, scaffolds and constructs were enzymatically digested with papain (125µg/ml - Sigma) in a buffer containing 100mM Sodium Phosphate (Sigma) with 5mM Na_2EDTA (Sigma) at pH 6.5 as previously described [43]. sGAG quantification was performed using a 1, 9 dimethylmethylene blue (DMMB) assay according to the manufacturer's protocol with bovine tracheal chondroitin 4- sulfate used as a reference standard (Blyscan sulfated sGAG assay kit, Biocolor, Northern Ireland). Quantification of dsDNA in the digested constructs was performed using a Quant-iT Pico Green dsDNA kit (Invitrogen) according to the manufacturer's protocol. The combination of results from the DMMB and pico-green assays provides a ratio of sGAG normalized to dsDNA content. Collagen content of scaffolds was quantified by measuring total hydroxyproline content as

previously described[9]. A hydroxyproline:collagen ratio of 1:7.69 was assumed to determine the collagen content [50].

2.7 Assessment of endotoxin contamination

ECM scaffolds were first tested for lipopolysaccharide (LPS) contamination using the HEK-Blue^{TM} hTLR4 assay system (Invivogen). HEK-blue cells (5 x 10^5 cells/ml) expressing TLR4 were stimulated with LPS (1–100 ng/ml; positive control), or ECM scaffolds for 24 h. The expression of SEAP which is under the control of NF-κB and AP-1 was tested by incubating cell supernatants with HEK-blue detection medium for 30 min at 37 °C and absorbance was read at 650 nm.

2.8 Analysis of cytokine production by macrophages upon seeding onto AC ECM derived scaffolds

Peripheral blood mononuclear cells (PBMC) were isolated by means of density gradient centrifugation from leukocyte-enriched buffy coats from anonymous healthy donors, obtained with permission from the Irish Blood Transfusion Board, St. James's Hospital, Dublin. $CD14^+$ myeloid cells were purified from PBMC by means of positive selection using anti-CD14 magnetic beads according to the manufacturer's protocol (Miltenyi Biotech, Bergisch Gladbach, Germany). Cells were shown to be >90% pure as determined by flow cytometry. $CD14^+$ monocytes were differentiated into macrophages for 6 days in the presence and absence of ECM derived scaffolds using M-CSF (50 ng/ml). As a positive control, macrophages were treated with 100 ng/ml Lipopolysaccharides (LPS) for 24 hours. IL-6, IL-8, TNFα and IL-10 cytokine production was quantified in cell supernatants by ELISA (eBiosciences).

2.9 Mechanical testing

Scaffolds (Φ5 mm x h 3 mm, n = 4) were subjected to a uniaxial unconfined compression test in PBS using a single column mechanical tester (Zwick/Roell Z2.5, Herefordshire, UK) with a 5N load cell. Briefly, constructs were kept hydrated in PBS bath maintained at room temperature. A preload of 0.01N was applied for 60 seconds to ensure that top and bottom construct surfaces were in direct contact with the impermeable loading platens. Force was zeroed after preload, then followed by a cyclic compression test consisting of 6 compressive cycles with increasing strain amplitude of 10, 20, 30, 40, 50 and 60% in sequence at a rate of 2.22% strain per second. A holding time of 10 seconds between each cycle was added to allow full height recovery of the samples. The load versus displacement data were recorded throughout. The apparent stress and strain were calculated by dividing the load value with the initial cross-sectional area of each sample and the displacement value with the initial sample height, respectively. Cumulative percentage of the total height loss and height loss per cycle was calculated to characterize the super-elastic properties of the constructs. Scaffold permanent deformation (PD) at each cycle was calculated as follows: PD = (Test Speed*Δt_n)/h_0, where Δt_n is the interval of time at the start of the n^{th} cycle in which no force is applied to the sample, while h_0 is the initial height of the sample. Samples were also subjected to 80% strain during 10 cycles at 2.22% strain per second (supplementary data). Differences between Young's modulus between 1^{st}, 5^{th} and 10^{th} cycle were compared to evaluate elasticity. Data was normalised to 1^{st} cycle in each group. To obtain the equilibrium modulus of cell-free scaffolds, stress relaxation tests were performed whereby 30% strain was applied followed by relaxation until equilibrium was achieved. For cell seeded constructs, 10% strain was applied during stress relaxation tests to obtain the equilibrium modulus. Immediately after this dynamic tests were performed by applying a cyclic strain of 1% at 1 Hz to determine the dynamic modulus of the engineered constructs.

2.10 Histology and immunohistochemistry

All samples were washed in PBS followed by overnight fixation in 4% paraformaldehyde (Sigma, Ireland). Samples were dehydrated and wax embedded. Embedded constructs were then sectioned at a thickness of 5µm using a microtome. Sections were stained with 1% alcian blue 8X in 0.1M HCl (Sigma, Ireland) to examine sulphated glycosaminoglycan (sGAG) and picrosirius red to examine collagen deposition. To identify the specific collagen types present in the constructs, immunohistochemistry was performed for collagen type I, type II or X as previously described [47]. Briefly, after dewaxing and rehydrating the sections antigen retrieval was performed by incubation with Chondrotinase ABC for collagen types I and II or with Pronase for collagen type X. After blocking for non-specific binding, sections were incubated with primary antibody (anti collagen type I (1:400), type II (1:100) or type X (1:200) all HRP-conjugated, all Abcam, UK) overnight at 4°C. Endogenous peroxidase activity was blocked with hydrogen peroxide (Sigma) prior to incubation with the anti-mouse IgG secondary antibody (Sigma). Sections were then incubated with 3,3'-diaminobenzidine (*DAB*) peroxidase substrate (Vector Labs, UK) to visualise positive staining.

2.11 Statistical analysis

All experiments were performed on three separate human donors. Results are presented as mean +/- standard deviation. Statistical analysis was performed using Graph Pad Prism (San Diego, USA). Statistical differences were analysed by one-way analysis of variance (ANOVA) with Tukey's test for multiple comparisons to compare experimental conditions. Statistically significant changes are marked as * = $p<0.05$; ** = $p\leq0.01$; *** = $p\leq0.001$

3. Results

3.1 ECM scaffold porosity, composition and mechanical properties

Highly elastic and porous scaffolds can be fabricated from pepsin solubilised cartilage ECM which have been cross-linked with glyoxal prior to freeze drying (Fig. 1). All scaffolds were found to display highly elastic mechanical properties when manually compressed (Fig. 1A), returning to their original shape after unloading. Histological and biochemical analysis of the solubilised ECM derived scaffolds demonstrated almost complete removal of sGAG from the matrix (Fig. 1 B&E), with strong staining for picrosirius red confirming the collagenous nature of the scaffolds. Collagen content was quantified by hydroxyproline assay, between 49% and 24% of the native dry weight of the collagen was maintained post scaffold fabrication (Fig. 1G). Scanning electron micrographs (SEM) of the scaffolds revealed a uniform pore architecture with the majority of pores having a diameter between 15-20μm (Fig. 1 B&C). All scaffolds were found to have a porosity between 97% and 98% (Fig. 1D). The amount of xenogeneic DNA remaining in the scaffolds post processing was also quantified. The mean quantity of DNA observed across all scaffolds tested was 39±1.5ng/mg of ECM dry weight (Fig. 1F).

Having fabricated four variations of highly elastic and porous scaffolds that had similar physical characteristics to each other, we then sought to mechanically evaluate the various scaffolds to ascertain if varying the concentrations of ECM and cross-linker can affect the mechanical properties of the resulting scaffolds. Mechanical testing of the scaffolds revealed that the concentration of cross-linker had no discernible effect on the mechanical properties of the scaffolds. Increasing the concentration of ECM in the scaffolds from 10mg/ml to 20mg/ml significantly increased the equilibrium modules. These scaffolds were also stiffer than those generated using traditional strategies of freeze-drying particulated articular cartilage ECM

slurry (AC-Cryomill) (Figure. 2A). To further evaluate the elastic properties of the scaffolds, a compression test consisting of 6 compressive cycles with increasing strain amplitude of 10, 20, 30, 40, 50 and 60% in succession was performed. A relatively elastic stress-strain response was observed at all amplitudes examined, with a small degree of hysteresis observed (Figure. 2B). Relatively minor levels of residual deformation were detected at the end of each loading cycle, which did accumulate with each loading cycle (Figure. 2B). Additional mechanical tests were also undertaken to demonstrate the different behaviour of solubilised ECM scaffolds and those produced using particulated ECM (AC-Cryomill). The solubilised ECM scaffolds were shown to undergo lower levels of permanent deformation after being compressed by 20% strain (Supp Fig.2A) and unlike the particulated ECM scaffolds, their stiffness did not reduce upon the application of high magnitude cyclic stain (Supp Fig.2B).

3.2 Chondrogenesis within solubilised ECM derived scaffolds

Having ascertained the physical, biochemical and mechanical properties of the scaffold variations, we next evaluated their chondrogenic-capacity by seeding them with FPSCs and maintaining the constructs in culture with TGF-β3. After 28 days in culture, all FPSC seeded scaffolds appeared cartilage-like in appearance, exhibiting a glossy structure (Fig. 3B). (Fig. 3A). All engineered tissues stained positive for alcian blue and picrosirius red, indicative of cartilage matrix synthesis. Similar histological staining of cell-free scaffolds is provided in Figure 1A. The most robust staining for new ECM deposition was observed for scaffolds fabricated using lower ECM (10mg) and lower glyoxal cross-linking (5mM) concentrations (Fig. 3B). Quantitative biochemical analysis substantiated the results observed histologically, with the 10mg/5mM scaffold supporting the highest levels of sGAG accumulation (GAG:DNA) of all groups examined (Fig. 3C-E). To confirm the development of cartilage-specific matrix within the ECM derived scaffolds, we next analysed the deposition of collagen

type I, II and X within the engineered tissues by immunohistochemistry (Figure 4). Type II collagen accumulation was observed in the 20mg/5mM, 10mg/10mM and 10mg/5mM groups, with little positive staining observed in the 20mg/10mM group. All engineered constructs stained weakly for collagen types I and X. To assess the mechanical properties of the engineered tissues after 28 days in culture, the constructs were subjected to unconfined compression testing to 10% strain. As expected the 10mg/5mM scaffold group, which supported the greatest levels of sGAG and type II collagen synthesis, were the stiffest constructs in terms of both equilibrium and dynamic modulus (Fig. 5 A&B)

3.3 Macrophage response to solubilised ECM

Having established that the 10mg/5mM scaffold best supported chondrogenesis of FPSCs, we next sought to evaluate the immune response to these optimized scaffolds. To first establish that the scaffold preparations were endotoxin (LPS) free, we tested the ECM scaffolds for LPS contamination and TLR4 activation as determined using the HEK-Blue LPS detection kit. We found that the concentration of endotoxin (LPS) was below the threshold level for TLR4 activation upon treatment with both native cartilage and solubilised AC ECM (Figure S1)

Immunogenicity of the native scaffolds was next assessed by culturing primary human macrophages in the presence of native cartilage or solubilised AC ECM. As a positive control, cells were stimulated with LPS to drive pro-inflammatory cytokine production. While particulated (cryomilled) articular cartilage promoted high levels of IL-6 production, this was reduced to control levels in the solubilised AC scaffold group (Fig. 6A) and there was a trend (albeit not significant) towards increased TNFα and IL-10 production (Fig. 6B & D). In contrast, no such increases were observed when macrophages were cultured with solubilised AC ECM. Interestingly**,** production of the chemokine, IL-8, was higher in the solubilized ECM scaffold versus particulated AC groups (Fig. 6C).

4. Discussion

The overall goal of this study was to fabricate a porous articular cartilage ECM derived scaffold that (i) was efficiently decellularized, (ii) was highly elastic with shape memory properties, (iii) facilitated the chondrogenic differentiation of adult stem cells and (iv) did not illicit a negative immune response when in contact with human macrophages. We developed four different scaffolds, with variations in the concentrations of ECM and degree of cross-linking, all of which were found to be sufficiently decellularized. The concentrations of ECM and glyoxal were chosen based on preliminary basic optimization experiments (data not shown) which examined cell infiltration and glyoxal toxicity. Glyoxal was chosen as a cross-linker due to the fact that it results in relatively low levels of cytotoxicity when compared to other aldehyde cross-linkers such as glutaraldehyde [40]. Scaffolds fabricated with 10mg/ml of AC-ECM crosslinked with 5mM glyoxal were found to promote the greatest deposition of sGAG and type II collagen by FPSCs. When cultured in the presence of macrophages, these scaffolds elicited an immune response believed more compatible with tissue regeneration (lower levels of the inflammatory cytokines IL-6 and TNF) when compared to non-decellularized, cryomilled AC scaffolds. However, we do note that IL-10 cytokine secretion was also decreased compared to native tissue. While this cytokine is considered an anti-inflammatory cytokine, and may be beneficial for the tissue regenerative process, the solubilisation protocol would appear to result in a reduction of global cytokine production rather than specifically reducing pro-inflammatory cytokines. Taken together, these results indicate that efficiently decellularized ECM derived scaffolds can be fabricated from solubilised porcine articular cartilage, and that these biomaterials are chondro-permissive.

Glyoxal cross-linking of the solubilised ECM produced elastic scaffolds exhibiting shape-memory properties. The solubilization process removed the majority of sGAGs from the

ECM, leaving behind a collagen rich solution. During the scaffold fabrication process, this solution is brought to neutral pH and 37^{o}C, leading to collagen fibril formation and gelation. Exposure to the dialdehyde glyoxal subsequently cross-links this physical network by crosslinking free amine groups in the collagen [37,51]. Freeze drying then produces a porous network of collagen struts displaying elastic properties at the macroscale. Previous mechanical tests on individual collagen fibrils has demonstrated that while they do not behave as homogenous materials, they commonly display linear behaviour, and can withstand tensile strains of up to 100% without fracturing [52]. The fibrils also exhibited time-dependent recoverable residual strains. Hence the elastic behaviour of these ECM derived scaffolds can be expected based on what is known about the mechanical properties of collagen itself. All scaffold variations demonstrated high elasticity when wet with shape-memory characteristics. In their current iteration the scaffolds should be capable of sustaining mechanically challenging environments due to their highly elastic properties, but will not initially contribute to load bearing until sufficient *de novo* tissue has formed. In order to improve mechanical properties of these scaffolds, different chemical crosslinking techniques could be employed such as EDAC/NHS crosslinking [9] or naturally derived crosslinking agents, such as genipin[53]. Additionally, the scaffolds could be reinforced with a polymeric (e.g. polycaprolactone) network or frame to provide additional mechanical support; [54] while this would increase the compressive modulus of the construct a reduction in elasticity would also result. Alternatively, the solubilized AC-ECM could be engineered into a methacrylated hydrogel which can be subsequently photo-crosslinked to create a construct that has previously been demonstrated to possess a compressive modulus approaching the range of native articular cartilage [12].

Having successfully fabricated the four scaffold variants, we then analysed the levels of xenogeneic DNA remaining in the scaffolds; 39 (+/-1.46) ng DNA per mg of dry weight was found to be the mean residual DNA level across the four variants. The AC solubilisation

procedure successfully removed ~95% of xenogeneic DNA from the biomaterial. This suggests that the resulting scaffolds are sufficiently decellularized for clinical use, based on established recommendations of <50 ng of DNA per mg of (dry weight) tissue [29]. Along with xenogenic DNA removal, the ultimate test to fully evaluate the effectiveness of decellularization protocol would be to employ the use of an *in vivo* model to assess the immune system response to the implant. Successful integration of ECM scaffolds is dependent on eliciting an appropriate host immune response [55]. Therefore preliminary assays were carried out to examine how primary human macrophages responded to these scaffolds. TNFα and IL-6 are potent pro-inflammatory cytokines produced by macrophages upon exposure to DNA or cellular antigens and were therefore examined as indicators of efficient decellularization. Non decellularized, cyromilled AC derived scaffolds enhanced production of both cytokines, however this was not observed in the solubilised AC derived scaffolds groups, suggesting that the solubilisation process was successful in removing most cellular antigens that would usually elicit a detrimental immune response. These cytokines, in addition to IL-10, are also normally enhanced in the presence of endotoxin, which can often contaminate biological scaffolds[56] The absence of any of these cytokines in the solubilised AC scaffold groups also indicates that scaffolds are produced free of any major endotoxin contamination. Furthermore, TNFα and IL-6 have been shown to inhibit chondrogenic differentiation of MSCs [57-59], therefore the decreased production of these cytokines provides further evidence that the solubilised AC scaffold will provide an environment supportive of chondrogenesis if implanted *in vivo*.

Interestingly, high levels of the chemokine IL-8 were produced by macrophages cultured in the presence of solubilised AC scaffolds compared to the non-decellularized, cyromilled AC scaffolds. The precise role of this chemokine in chondrogenesis has not yet been established, however IL-8 in the presence of bone marrow concentrate has been shown to upregulate the

chondrogenic markers Sox9, ACAN and Col II in MSCs [60] . It will be interesting to determine the precise role played by this chemokine in host interactions with ECM scaffolds. Of note, it has been shown that IL-8 can also promote osteoclastogenesis [61], therefore a certain level of this protein may actually be beneficial for optimal remodelling if such biomaterials were used for osteochondral defect repair.

Solubilised cartilage ECM derived scaffolds were found to facilitate robust chondrogenic differentiation of FPSCs. Adult stem cells have been isolated from several tissues including the bone marrow, [62-64] subcutaneous adipose tissue [65,66] and the infrapatellar fat pad (IFP) [8-10,45,47,67]. MSCs from these tissues have been demonstrated to readily differentiate into cartilage tissue and as such have been proposed as an ideal cell source for cartilage repair applications [68]. While less studied than bone marrow-derived MSCs, both the anatomical location of the IFP and the high proportion of progenitor cells found in the tissue make the IFP an ideal cell source for cartilage repair applications. Infrapatellar fat pad-derived stromal cells (FPSCs) have been demonstrated to have at least comparable chondrogenic capacity to bone marrow derived-MSCs [69-71]. Scaffolds fabricated with 10mg/ml of AC-ECM crosslinked with 5mM glyoxal were found to promote the greatest deposition type II collagen by FPSCs within the constructs. Type II collagen is a key marker of chondrogenic differentiation of FPSCs towards a "hyaline-like" phenotype. All scaffold variants demonstrated low levels of type I collagen deposition, a marker of fibro-cartilaginous differentiation and weak staining for type X collagen, a marker of hypertrophic differentiation. This collagen deposition profile is typical for FPSCs which generally undergo attenuated hypertrophic differentiation when compared to bone marrow derived MSCs [72]. The correlation between increase sGAG production and decreased AC-ECM and glyoxal concentrations may be a result of a greater interconnectivity of internal pores, allowing for greater cell infiltration to the centre of the scaffold[73-75]. This hypothesis may explain the more robust, uniform sGAG staining observed in the 10mg/ml –

5mM scaffolds. Alteration of the freeze drying kinetics used or other methods to increase the pore size of these scaffold may further enhance the chondro-inductivity of the scaffolds.

The 10mg/5mM scaffold promoted the development of the stiffest cartilaginous tissue after 28 days in culture. This scaffold also supported the highest levels of sGAG deposition, with previous studies confirming a strong correlation between sGAG deposition and the equilibrium and dynamic moduli in FPSC-derived engineered cartilage tissues [70]. Traditionally, AC-ECM scaffolds have been fabricated from particulated (usually cyromilled) AC, mixed with water to form a slurry and then freeze dried to form a scaffold. These scaffolds would generally maintain the majority of GAGs within the matrix, unlike the solubilized AC-ECM scaffolds we have developed here. Their overall porosity is typically lower than solubilised ECM scaffolds, although the mean pore size is typically higher. Previous work from our laboratory has explored the use of such particulated AC-ECM scaffolds for cartilage tissue engineering, using human FPSCs from the same donor, as well as the same seeding density, scaffold size and time-point (28 days), allowing us to compare the matrix deposited in both scaffold types. Both scaffold types supported the robust chondrogenic differentiation of FPSCs, with slightly higher levels of sGAG deposition within the particulated (cyromilled) scaffolds (120μg Vs. 115μg GAG per scaffold respectively) after 28 days in culture[10]. It should be noted, however, that the particulated scaffolds used in that study were not decellularized and lack the elastic properties of the solubilized and glyoxal cross-linked AC-ECM scaffolds (See Supplementary Fig. 2)

It should be noted that the mechanical properties of the generated cartilaginous tissues described in this study are significantly lower than the properties of native articular cartilage, which has a compressive modules of 0.1 to 2 MPa [76]. Therefore, if the proposed scaffold is to be used for the *in vitro* engineering of functional cartilage grafts for subsequent implantation, further optimization of the culture conditions and/or the scaffold design may be required. In

conclusion, this study details the successful fabrication of porous articular cartilage ECM derived scaffolds, which were sufficiently decellularized for putative clinical use, did not elicit a potentially detrimental immunological response *in vitro* and were shown to promote robust chondrogenic differentiation of FPSCs. Due to the characteristics presented here, these scaffolds have the potential to be used in clinical applications, either in combination with current microfracture techniques, or seeded with cells prior to implantation, in order to treat focal cartilage defects.

Acknowledgements

Funding for the project was received from Enterprise Ireland (CF/2014/4325), Science Foundation Ireland through the Investigators Programme (12/IA/1554) and by the European Research Council (ANCHOR – 779909, StemRepair -258463 and JointPrinting – 647004). This research was co-funded by the European Regional Development Fund (ERDF) under Ireland's European Structural and Investment Funds Programmes 2014-2020.

References

1. Buckwalter J, Mow V, Ratcliffe A. Restoration of Injured or Degenerated Articular Cartilage. Journal of the American Academy of Orthopaedic Surgeons 1994;2(4):192-201.
2. Smith BD, Grande DA. The current state of scaffolds for musculoskeletal regenerative applications. Nature Reviews Rheumatology 2015;11(4):213-222.
3. Daher RJ, Chahine NO, Greenberg AS, Sgaglione NA, Grande DA. New methods to diagnose and treat cartilage degeneration. Nature Reviews Rheumatology 2009;5(11):599-607.
4. Knutsen G, Engebretsen L, Ludvigsen TC, Drogset JO, Grøntvedt T, Solheim E, Strand T, Roberts S, Isaksen V, Johansen O. Autologous chondrocyte implantation compared with microfracture in the kneeA randomized trial. The Journal of Bone & Joint Surgery 2004;86(3):455-464.
5. Badylak SF, Freytes DO, Gilbert TW. Extracellular matrix as a biological scaffold material: Structure and function. Acta Biomaterialia 2009;5(1):1-13.
6. Badylak SF. The extracellular matrix as a biologic scaffold material. Biomaterials 2007;28(25):3587-3593.
7. Sutherland AJ, Converse GL, Hopkins RA, Detamore MS. The Bioactivity of Cartilage Extracellular Matrix in Articular Cartilage Regeneration. Advanced Healthcare Materials 2015;4(1):29-39.
8. Almeida HV, Eswaramoorthy R, Cunniffe GM, Buckley CT, O'Brien FJ, Kelly DJ. Fibrin hydrogels functionalized with cartilage extracellular matrix and incorporating freshly isolated stromal cells as an injectable for cartilage regeneration. Acta Biomaterialia 2016;36:55-62.
9. Almeida HV, Liu Y, Cunniffe GM, Mulhall KJ, Matsiko A, Buckley CT, O'Brien FJ, Kelly DJ. Controlled release of transforming growth factor-β3 from cartilage-extra-cellular-matrix-derived scaffolds to promote chondrogenesis of human-joint-tissue-derived stem cells. Acta biomaterialia 2014;10(10):4400-4409.
10. Almeida HV, Cunniffe GM, Vinardell T, Buckley CT, O'Brien FJ, Kelly DJ. Coupling Freshly Isolated CD44+ Infrapatellar Fat Pad-Derived Stromal Cells with a TGF-β3 Eluting Cartilage ECM-Derived Scaffold as a Single-Stage Strategy for Promoting Chondrogenesis. Advanced healthcare materials 2015;4(7):1043-1053.
11. Cheng N-C, Estes BT, Awad HA, Guilak F. Chondrogenic differentiation of adipose-derived adult stem cells by a porous scaffold derived from native articular cartilage extracellular matrix. Tissue Engineering Part A 2008;15(2):231-241.
12. Beck EC, Barragan M, Tadros MH, Gehrke SH, Detamore MS. Approaching the compressive modulus of articular cartilage with a decellularized cartilage-based hydrogel. Acta Biomaterialia 2016;38:94-105.
13. Vindas Bolaños RA, Cokelaere SM, Estrada McDermott JM, Benders KEM, Gbureck U, Plomp SGM, Weinans H, Groll J, van Weeren PR, Malda J. The use of a cartilage decellularized matrix scaffold for the repair of osteochondral defects: the importance of long-term studies in a large animal model. Osteoarthritis and Cartilage 2017;25(3):413-420.
14. Sutherland AJ, Beck EC, Dennis SC, Converse GL, Hopkins RA, Berkland CJ, Detamore MS. Decellularized Cartilage May Be a Chondroinductive Material for Osteochondral Tissue Engineering. PLOS ONE 2015;10(5):e0121966.
15. Yang Q, Peng J, Guo Q, Huang J, Zhang L, Yao J, Yang F, Wang S, Xu W, Wang A and others. A cartilage ECM-derived 3-D porous acellular matrix scaffold for in vivo cartilage tissue engineering with PKH26-labeled chondrogenic bone marrow-derived mesenchymal stem cells. Biomaterials 2008;29(15):2378-2387.
16. Beck EC, Barragan M, Libeer TB, Kieweg SL, Converse GL, Hopkins RA, Berkland CJ, Detamore MS. Chondroinduction from Naturally Derived Cartilage Matrix: A Comparison Between

Devitalized and Decellularized Cartilage Encapsulated in Hydrogel Pastes. Tissue Engineering. Part A 2016;22(7-8):665-679.
17. Benders K, Boot W, Cokelaere S, Van Weeren P, Gawlitta D, Bergman H, Saris DB, Dhert W, Malda J. Multipotent stromal cells outperform chondrocytes on cartilage-derived matrix scaffolds. Cartilage 2014;5(4):221-230.
18. Cunniffe GM, Díaz-Payno PJ, Sheehy EJ, Critchley SE, Almeida HV, Pitacco P, Carroll SF, Mahon OR, Dunne A, Levingstone TJ and others. Tissue-specific extracellular matrix scaffolds for the regeneration of spatially complex musculoskeletal tissues. Biomaterials 2019;188:63-73.
19. Gawlitta D, Benders KEM, Visser J, van der Sar AS, Kempen DHR, Theyse LFH, Malda J, Dhert WJA. Decellularized Cartilage-Derived Matrix as Substrate for Endochondral Bone Regeneration. Tissue Engineering Part A 2014;21(3-4):694-703.
20. Almeida HV, Sathy BN, Dudurych I, Buckley CT, O'Brien FJ, Kelly DJ. Anisotropic Shape-Memory Alginate Scaffolds Functionalized with Either Type I or Type II Collagen for Cartilage Tissue Engineering. Tissue Engineering Part A 2017;23(1-2):55-68.
21. Zheng X, Yang F, Wang S, Lu S, Zhang W, Liu S, Huang J, Wang A, Yin B, Ma N and others. Fabrication and cell affinity of biomimetic structured PLGA/articular cartilage ECM composite scaffold. Journal of Materials Science: Materials in Medicine 2011;22(3):693-704.
22. Jia S, Liu L, Pan W, Meng G, Duan C, Zhang L, Xiong Z, Liu J. Oriented cartilage extracellular matrix-derived scaffold for cartilage tissue engineering. Journal of Bioscience and Bioengineering 2012;113(5):647-653.
23. Schwarz S, Koerber L, Elsaesser AF, Goldberg-Bockhorn E, Seitz AM, Dürselen L, Ignatius A, Walther P, Breiter R, Rotter N. Decellularized cartilage matrix as a novel biomatrix for cartilage tissue-engineering applications. Tissue engineering Part A 2012;18(21-22):2195-2209.
24. Luo L, Eswaramoorthy R, Mulhall KJ, Kelly DJ. Decellularization of porcine articular cartilage explants and their subsequent repopulation with human chondroprogenitor cells. Journal of the mechanical behavior of biomedical materials 2016;55:21-31.
25. Fermor HL, Russell SL, Williams S, Fisher J, Ingham E. Development and characterisation of a decellularised bovine osteochondral biomaterial for cartilage repair. Journal of Materials Science: Materials in Medicine 2015;26(5):186.
26. Badylak SF, Gilbert TW. Immune response to biologic scaffold materials. Seminars in Immunology 2008;20(2):109-116.
27. Keane TJ, Badylak SF. The host response to allogeneic and xenogeneic biological scaffold materials. Journal of tissue engineering and regenerative medicine 2015;9(5):504-511.
28. Brown BN, Valentin JE, Stewart-Akers AM, McCabe GP, Badylak SF. Macrophage phenotype and remodeling outcomes in response to biologic scaffolds with and without a cellular component. Biomaterials 2009;30(8):1482-1491.
29. Crapo PM, Gilbert TW, Badylak SF. An overview of tissue and whole organ decellularization processes. Biomaterials 2011;32(12):3233-3243.
30. Benders KEM, Weeren PRv, Badylak SF, Saris DBF, Dhert WJA, Malda J. Extracellular matrix scaffolds for cartilage and bone regeneration. Trends in Biotechnology 2013;31(3):169-176.
31. Rowland CR, Lennon DP, Caplan AI, Guilak F. The effects of crosslinking of scaffolds engineered from cartilage ECM on the chondrogenic differentiation of MSCs. Biomaterials 2013;34(23):5802-5812.
32. Haugh MG, Jaasma MJ, O'Brien FJ. The effect of dehydrothermal treatment on the mechanical and structural properties of collagen-GAG scaffolds. Journal of biomedical materials research Part A 2009;89(2):363-369.
33. Gao S, Yuan Z, Guo W, Chen M, Liu S, Xi T, Guo Q. Comparison of glutaraldehyde and carbodiimides to crosslink tissue engineering scaffolds fabricated by decellularized porcine menisci. Materials Science and Engineering: C 2017;71:891-900.

34. Gough JE, Scotchford CA, Downes S. Cytotoxicity of glutaraldehyde crosslinked collagen/poly(vinyl alcohol) films is by the mechanism of apoptosis. Journal of Biomedical Materials Research 2002;61(1):121-130.
35. Böer U, Schridde A, Anssar M, Klingenberg M, Sarikouch S, Dellmann A, Harringer W, Haverich A, Wilhelmi M. The immune response to crosslinked tissue is reduced in decellularized xenogeneic and absent in decellularized allogeneic heart valves. The International journal of artificial organs 2015;38(4):199-209.
36. Brown BN, Badylak SF. Extracellular matrix as an inductive scaffold for functional tissue reconstruction. Translational Research 2014;163(4):268-285.
37. Wang L, Stegemann JP. Glyoxal crosslinking of cell-seeded chitosan/collagen hydrogels for bone regeneration. Acta Biomaterialia 2011;7(6):2410-2417.
38. Herbage D, Bouillet J, Bernengo JC. Biochemical and physiochemical characterization of pepsin-solubilized type-II collagen from bovine articular cartilage. Biochemical Journal 1977;161(2):303-312.
39. Deyl Z, Mikšık I, Eckhardt A. Preparative procedures and purity assessment of collagen proteins. Journal of Chromatography B 2003;790(1):245-275.
40. Kieć-Swierczyńska M, Krecisz B, Krysiak B, Kuchowicz E, Rydzyński KJIJoOM, Health E. Occupational allergy to aldehydes in health care workers. Clinical observations. Experiments. 1998;11(4):349-358.
41. Karageorgiou V, Kaplan D. Porosity of 3D biomaterial scaffolds and osteogenesis. Biomaterials 2005;26(27):5474-5491.
42. Loh QL, Choong C. Three-Dimensional Scaffolds for Tissue Engineering Applications: Role of Porosity and Pore Size. Tissue Engineering Part B: Reviews 2013;19(6):485-502.
43. Almeida HV, Mulhall KJ, O'Brien FJ, Kelly DJ. Stem cells display a donor dependent response to escalating levels of growth factor release from extracellular matrix-derived scaffolds. Journal of Tissue Engineering and Regenerative Medicine 2016.
44. Liu Y, Buckley CT, Mulhall KJ, Kelly DJ. Combining BMP-6, TGF-β3 and hydrostatic pressure stimulation enhances the functional development of cartilage tissues engineered using human infrapatellar fat pad derived stem cells. Biomaterials Science 2013;1(7):745-752.
45. O'hEireamhoin S, Buckley CT, Jones E, McGonagle D, Mulhall KJ, Kelly DJ. Recapitulating aspects of the oxygen and substrate environment of the damaged joint milieu for stem cell-based cartilage tissue engineering. Tissue Engineering Part C: Methods 2012;19(2):117-127.
46. Liu Y, Buckley CT, Downey R, Mulhall KJ, Kelly DJ. The Role of Environmental Factors in Regulating the Development of Cartilaginous Grafts Engineered Using Osteoarthritic Human Infrapatellar Fat Pad–Derived Stem Cells. Tissue Engineering Part A 2012;18(15-16):1531-1541.
47. Buckley CT, Vinardell T, Thorpe SD, Haugh MG, Jones E, McGonagle D, Kelly DJ. Functional properties of cartilaginous tissues engineered from infrapatellar fat pad-derived mesenchymal stem cells. Journal of Biomechanics 2010;43(5):920-926.
48. Buckley CT, Vinardell T, Kelly DJ. Oxygen tension differentially regulates the functional properties of cartilaginous tissues engineered from infrapatellar fat pad derived MSCs and articular chondrocytes. Osteoarthritis and Cartilage 2010;18(10):1345-1354.
49. Buckley CT, Kelly DJ. Expansion in the presence of FGF-2 enhances the functional development of cartilaginous tissues engineered using infrapatellar fat pad derived MSCs. Journal of the Mechanical Behavior of Biomedical Materials 2012;11:102-111.
50. Ignat'eva NY, Danilov NA, Averkiev SV, Obrezkova MV, Lunin VV, Sobol' EN. Determination of hydroxyproline in tissues and the evaluation of the collagen content of the tissues. Journal of Analytical Chemistry 2007;62(1):51-57.
51. Rao RR, Peterson AW, Ceccarelli J, Putnam AJ, Stegemann JP. Matrix composition regulates three-dimensional network formation by endothelial cells and mesenchymal stem cells in collagen/fibrin materials. Angiogenesis 2012;15(2):253-264.

52. Shen ZL, Dodge MR, Kahn H, Ballarini R, Eppell SJ. Stress-Strain Experiments on Individual Collagen Fibrils. Biophysical Journal 2008;95(8):3956-3963.
53. Pinheiro A, Cooley A, Liao J, Prabhu R, Elder S. Comparison of natural crosslinking agents for the stabilization of xenogenic articular cartilage. Journal of Orthopaedic Research 2016;34(6):1037-1046.
54. Daly AC, Cunniffe GM, Sathy BN, Jeon O, Alsberg E, Kelly DJ. 3D Bioprinting of Developmentally Inspired Templates for Whole Bone Organ Engineering. Advanced Healthcare Materials 2016;5(18):2353-2362.
55. Gilbert TW. Strategies for tissue and organ decellularization. Journal of cellular biochemistry 2012;113(7):2217-2222.
56. Rossol M, Heine H, Meusch U, Quandt D, Klein C, Sweet MJ, Hauschildt SJCRiI. LPS-induced cytokine production in human monocytes and macrophages. 2011;31(5).
57. Wei H, Shen G, Deng X, Lou D, Sun B, Wu H, Long L, Ding T, Zhao J. The role of IL-6 in bone marrow (BM)-derived mesenchymal stem cells (MSCs) proliferation and chondrogenesis. Cell and tissue banking 2013;14(4):699-706.
58. Nakajima S, Naruto T, Miyamae T, Imagawa T, Mori M, Nishimaki S, Yokota S. Interleukin-6 inhibits early differentiation of ATDC5 chondrogenic progenitor cells. Cytokine 2009;47(2):91-97.
59. Wehling N, Palmer G, Pilapil C, Liu F, Wells J, Müller P, Evans CH, Porter R. Interleukin-1β and tumor necrosis factor α inhibit chondrogenesis by human mesenchymal stem cells through NF-κB–dependent pathways. Arthritis & Rheumatology 2009;60(3):801-812.
60. Yoon DS, Lee K-M, Kim S-H, Kim SH, Jung Y, Kim SH, Park KH, Choi Y, Ryu HA, Choi WJ. Synergistic action of IL-8 and bone marrow concentrate on cartilage regeneration through upregulation of chondrogenic transcription factors. Tissue Engineering Part A 2016;22(3-4):363-374.
61. Kopesky P, Tiedemann K, Alkekhia D, Zechner C, Millard B, Schoeberl B, Komarova SV. Autocrine signaling is a key regulatory element during osteoclastogenesis. Biology open 2014:BIO20148128.
62. Friedenstein AJ, Piatetzky S, II, Petrakova KV. Osteogenesis in transplants of bone marrow cells. J Embryol Exp Morphol 1966;16(3):381-90.
63. Owen M, Friedenstein A. Stromal stem cells: marrow-derived osteogenic precursors. Cell and molecular biology of vertebrate hard tissues 1988;136:42-60.
64. Johnstone B, Hering TM, Caplan AI, Goldberg VM, Yoo JU. In VitroChondrogenesis of Bone Marrow-Derived Mesenchymal Progenitor Cells. Experimental Cell Research 1998;238(1):265-272.
65. Zuk PA, Zhu M, Ashjian P, De Ugarte DA, Huang JI, Mizuno H, Alfonso ZC, Fraser JK, Benhaim P, Hedrick MH. Human adipose tissue is a source of multipotent stem cells. Molecular Biology of the Cell 2002;13(12):4279-4295.
66. Guilak F, Estes BT, Diekman BO, Moutos FT, Gimble JM. 2010 Nicolas Andry Award: Multipotent Adult Stem Cells from Adipose Tissue for Musculoskeletal Tissue Engineering. Clinical Orthopaedics and Related Research 2010;468(9):2530-2540.
67. Wickham MQ, Erickson GR, Gimble JM, Vail TP, Guilak F. Multipotent Stromal Cells Derived From the Infrapatellar Fat Pad of the Knee. Clinical Orthopaedics and Related Research 2003;412:196-212.
68. Garcia J, Mennan C, McCarthy HS, Roberts S, Richardson JB, Wright KT. Chondrogenic Potency Analyses of Donor-Matched Chondrocytes and Mesenchymal Stem Cells Derived from Bone Marrow, Infrapatellar Fat Pad, and Subcutaneous Fat. Stem Cells International 2016;2016:11.
69. Carroll SF, Buckley CT, Kelly DJ. Cyclic hydrostatic pressure promotes a stable cartilage phenotype and enhances the functional development of cartilaginous grafts engineered

using multipotent stromal cells isolated from bone marrow and infrapatellar fat pad. Journal of Biomechanics 2014;47(9):2115-2121.
70. Vinardell T, Buckley CT, Thorpe SD, Kelly DJ. Composition–function relations of cartilaginous tissues engineered from chondrocytes and mesenchymal stem cells isolated from bone marrow and infrapatellar fat pad. Journal of Tissue Engineering and Regenerative Medicine 2011;5(9):673-683.
71. Ding D-C, Wu K-C, Chou H-L, Hung W-T, Liu H-W, Chu T-Y. Human Infrapatellar Fat Pad-Derived Stromal Cells Have More Potent Differentiation Capacity Than Other Mesenchymal Cells and Can Be Enhanced by Hyaluronan. Cell Transplantation 2015;24(7):1221-1232.
72. Vinardell T, Sheehy EJ, Buckley CT, Kelly DJ. A comparison of the functionality and in vivo phenotypic stability of cartilaginous tissues engineered from different stem cell sources. Tissue Engineering Part A 2012;18(11-12):1161-1170.
73. Amos M, P. GJ, J. OBF. Scaffold Mean Pore Size Influences Mesenchymal Stem Cell Chondrogenic Differentiation and Matrix Deposition. 2015;21(3-4):486-497.
74. Sohier J, Moroni L, Blitterswijk Cv, Groot Kd, Bezemer JJEoodd. Critical factors in the design of growth factor releasing scaffolds for cartilage tissue engineering. 2008;5(5):543-566.
75. Hollister SJ. Porous scaffold design for tissue engineering. Nature Materials 2005;4(7):518-524.
76. Mow VC, Guo XE. Mechano-electrochemical properties of articular cartilage: their inhomogeneities and anisotropies. Annual Review of Biomedical Engineering 2002;4(1):175-209.

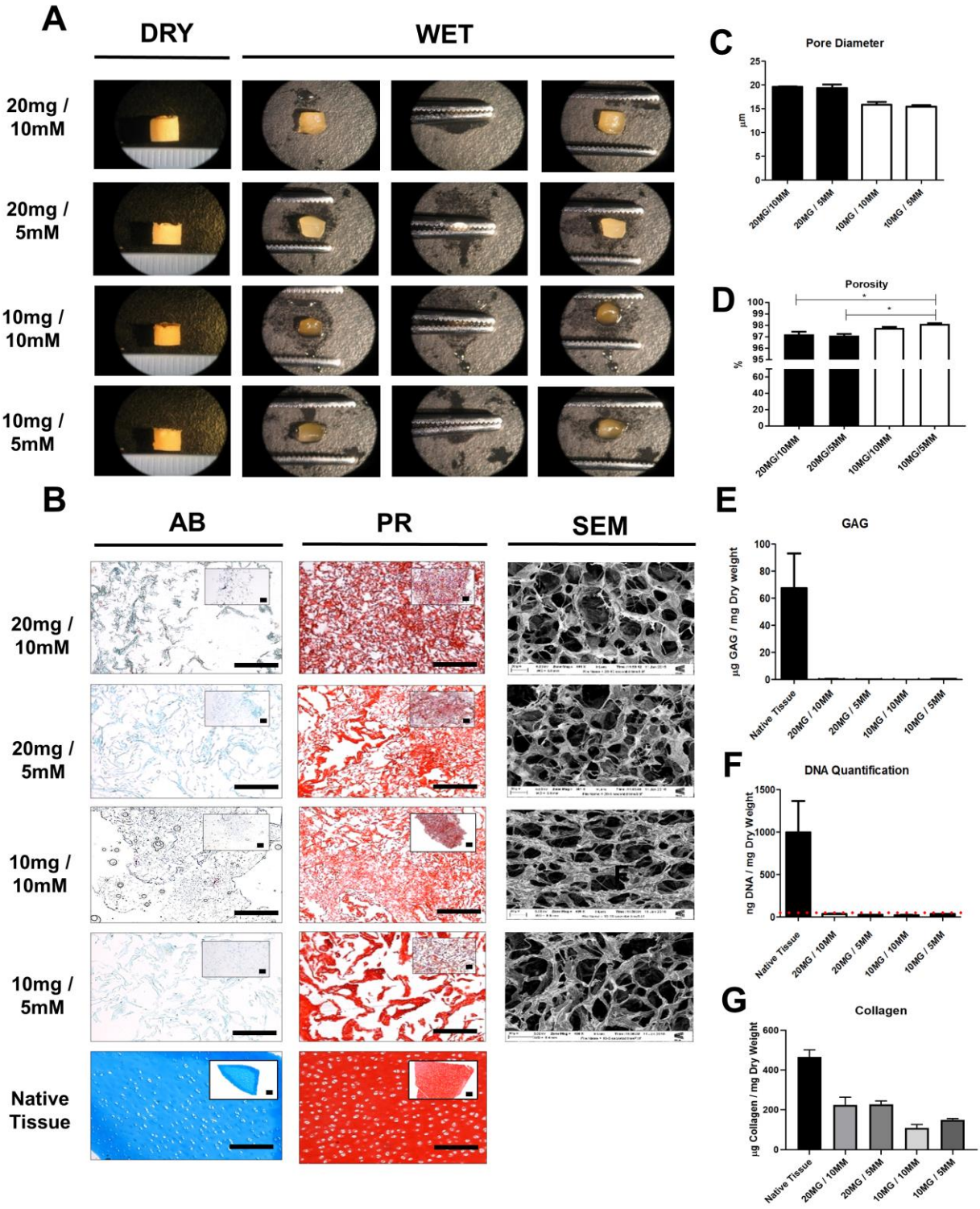

Figure 1: Characterisation of solubilised ECM derived scaffolds. Visualisation of the physical characteristics of the cell free ECM derived scaffolds was obtained by stereoscopic photography, histological staining and scanning electron microscopy (SEM) (A+B). Scaffolds contained either 10mg or 20mg of solubilised ECM, cross-linked with either 5mM or 10mM glyoxal. Mean pore diameter (C) and scaffold porosity (D) was obtained from 4 scaffolds per

group. sGAG (E),DNA (F) collagen (G) levels of scaffolds were quantified by biochemical assay (n=4). Dashed line in F represents 50ng/mg sufficient decellularization threshold. Scale bar =200µm in histological images and 20µm in SEM images. AB= Alcian Blue, PR= Picrosirius Red.* $P \leq 0.05$, ** $P \leq 0.01$ and *** $P \leq 0.001$.

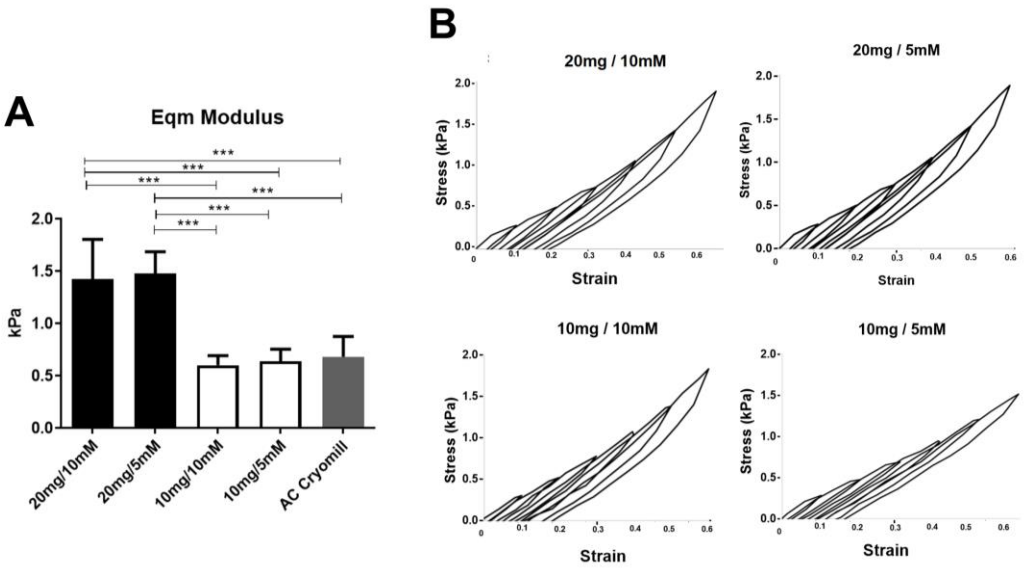

Figure 2: Mechanical properties of solubilised AC-ECM scaffolds. To obtain the cell free AC-ECM scaffold equilibrium modulus, stress relaxation tests were performed whereby 30% strain was applied to the samples (A). All scaffolds tested demonstrated elastic properties as visualised by the stress strain curves (B). *** $P \leq 0.001$, n=4. Scaffolds contained either 10mg or 20mg of solubilised ECM, cross-linked with either 5mM or 10mM glyoxal.

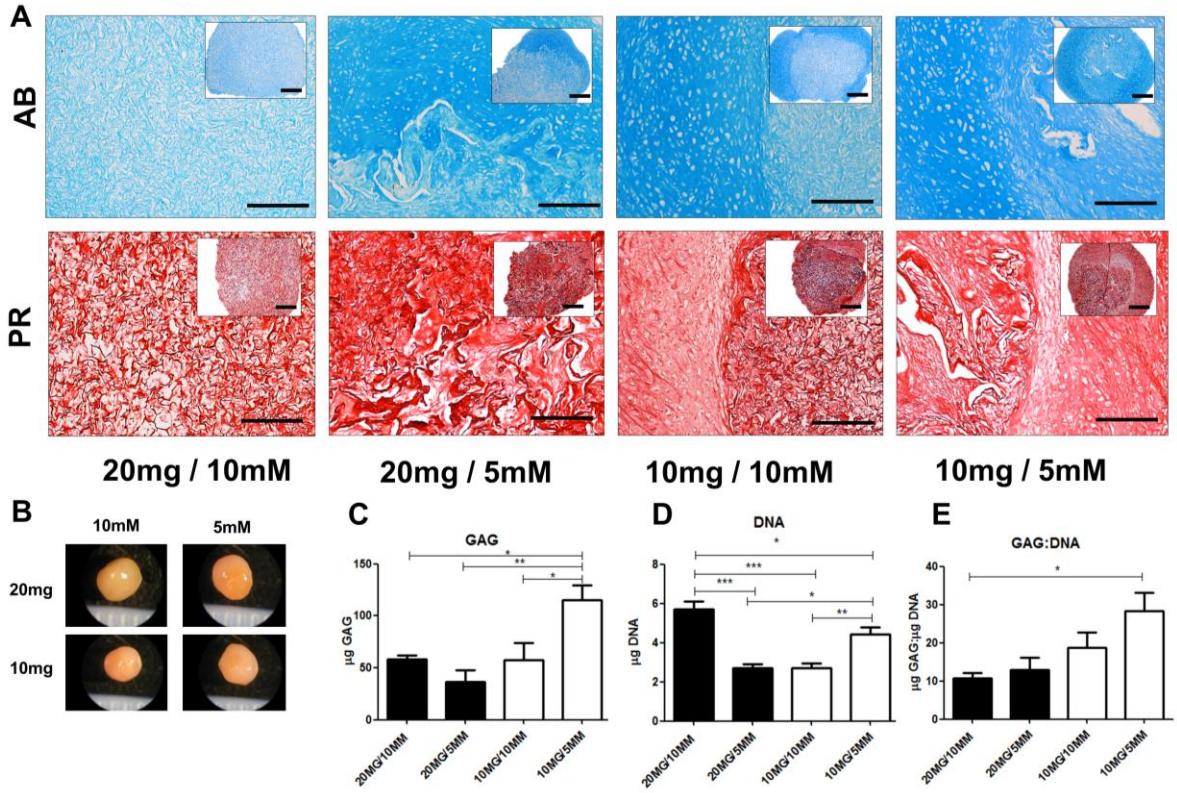

Figure 3: Robust chondrogenesis observed in 10mg / 5mM AC-ECM scaffolds after 28 days *in vitro*. sGAG and collagen was deposited by FPSCs in all scaffold groups (A). Stereoscopic micrographs show cartilage-like tissue formation in all groups, indentations on scale bar =1mm (B). Biochemical quantification revels the greatest sGAG deposition in the 10mg / 5mM group (C-E). Scale bar =200µm. AB= Alcian Blue, PR= Picrosirius Red. * $P \leq 0.05$, ** $P \leq 0.01$ and *** $P \leq 0.001$. Combined results from 3 individual donors, n=4 per donor.

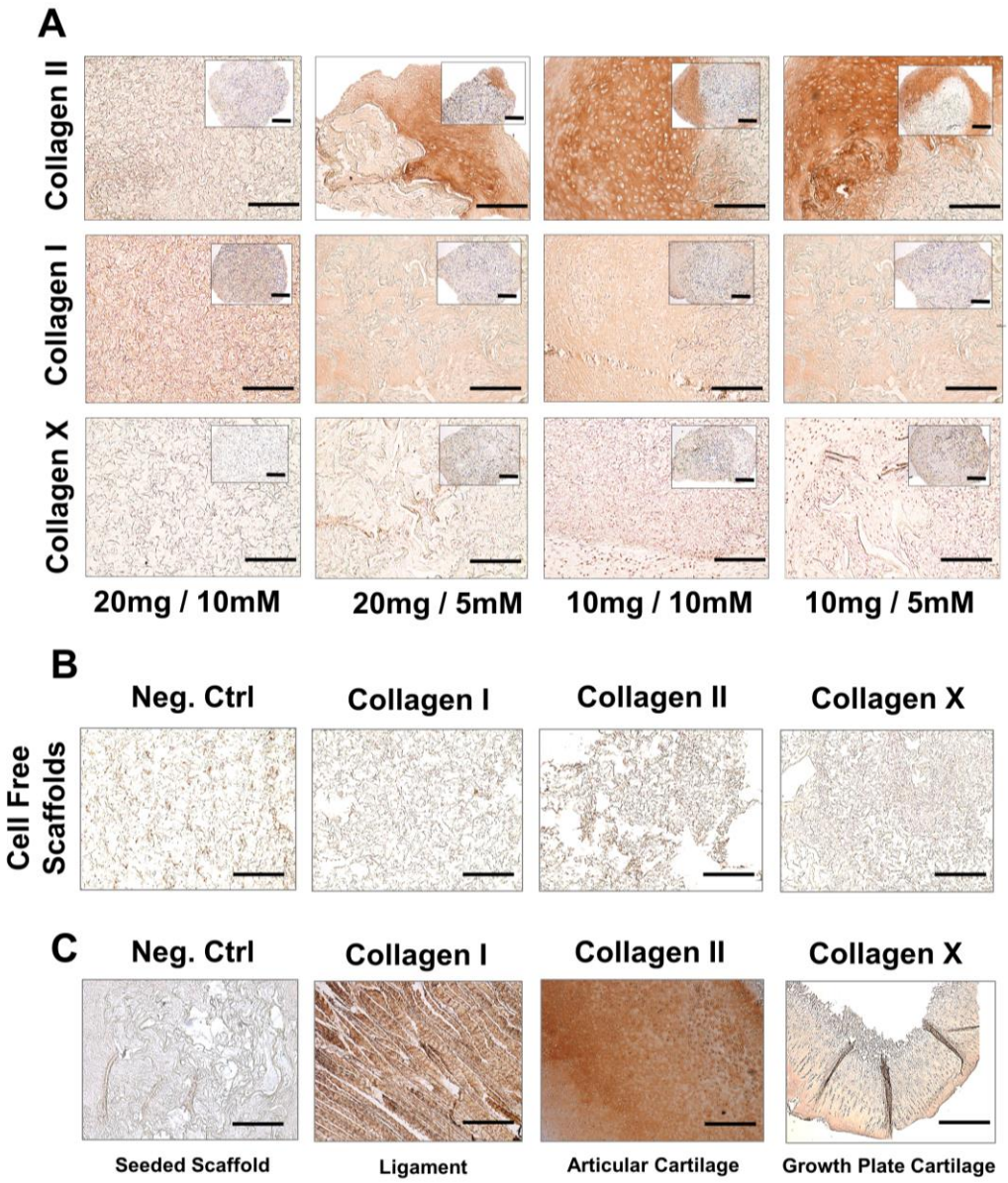

Figure 4: AC-ECM scaffolds seeded with FPSCs immunohistochemical analysis. Immunohistochemical analysis revealed that 20mg / 5mM, 10mg / 10mM and 10mg / 5mM groups all deposited type II collagen after 28 days. Also collagen deposition typical of differentiating FPSCs was observed, that is low deposition of type I collagen and type X collagen (A). Cell free scaffolds were subjected to the same immunohistochemistry procedure as in A to demonstrate no positive staining was present prior to cell seeding. Negative control images are without primary antibody only (B&C). Tissue specific positive controls for immunohistochemistry demonstrate positive staining for collagen types I, II and X in ligament, AC and growth plate cartilage respectively (C) Scale bar =200µm

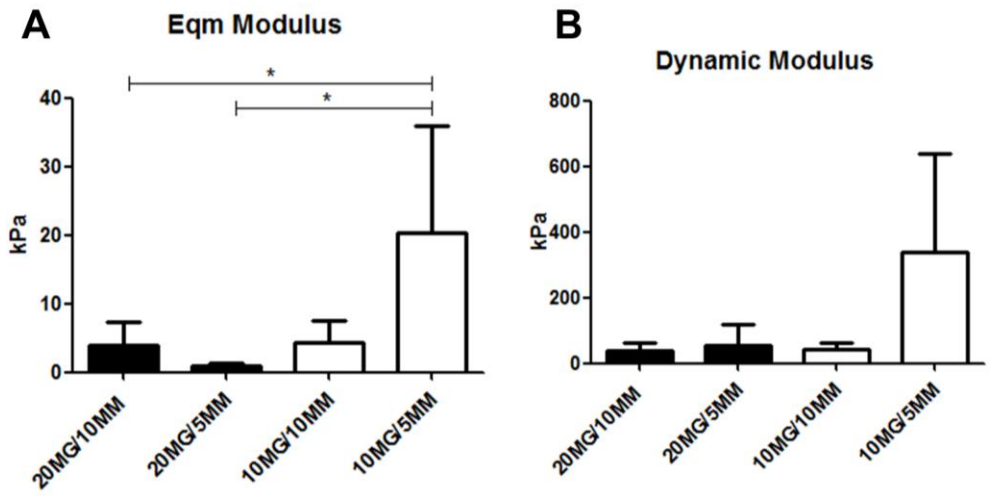

Figure 5: Mechanical properties of cell seeded AC-ECM scaffolds after 28 days *in vitro*. To obtain the cell seeded AC-ECM scaffold equilibrium modulus, stress relaxation tests were performed whereby 10% strain was applied to the samples (A). Dynamic modulus was obtained by applying a cyclic strain of 1% at 1 Hz to the scaffolds (B). Combined results from 3 individual donors, n=4 per donor. * $P \leq 0.05$.

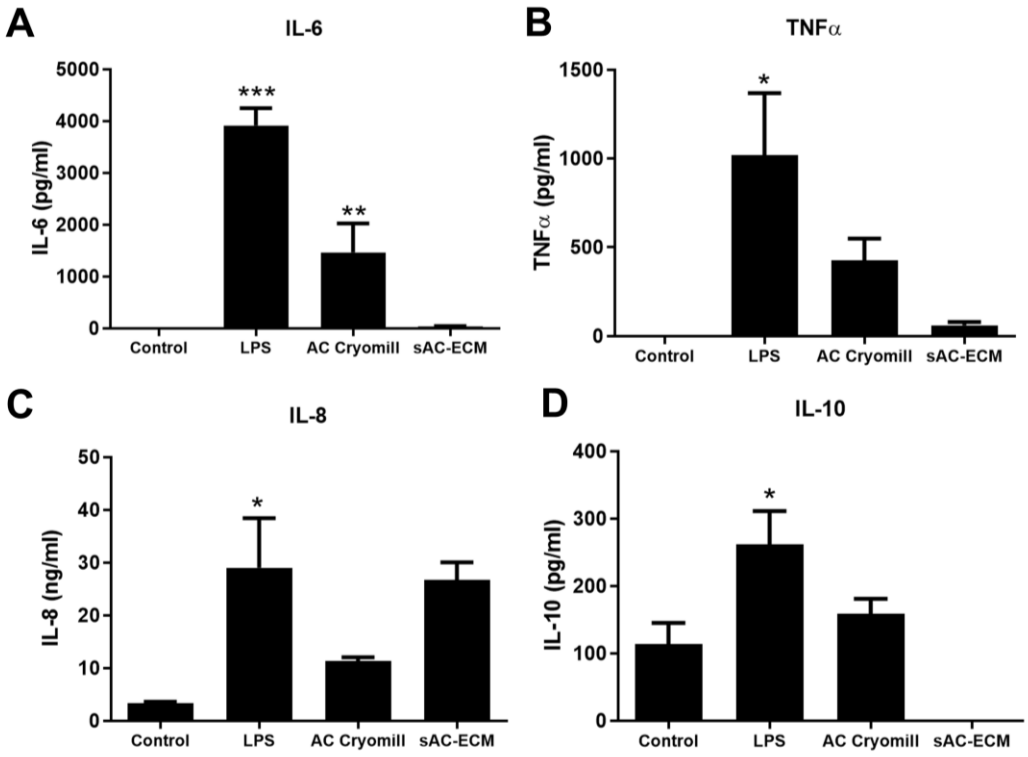

Figure 6: Effect of decellularisation of IL-6, TNFα, IL-8 and IL-10 cytokine production. Primary human macrophages (1 x 10^6 cells/ml) were treated with native or solubilised articular cartilage for 24 hours. As a positive control, macrophages were treated with 100 ng/ml LPS for 24 hours. (A) IL-6, (B) TNFα, (C) IL-8 and (D) IL-10 cytokine production was quantified in cell supernatants by ELISA. Unstimulated macrophages are the control group in all assays. Results shown are means (± SD) for triplicate cultures and are representative of 3 independent experiments.

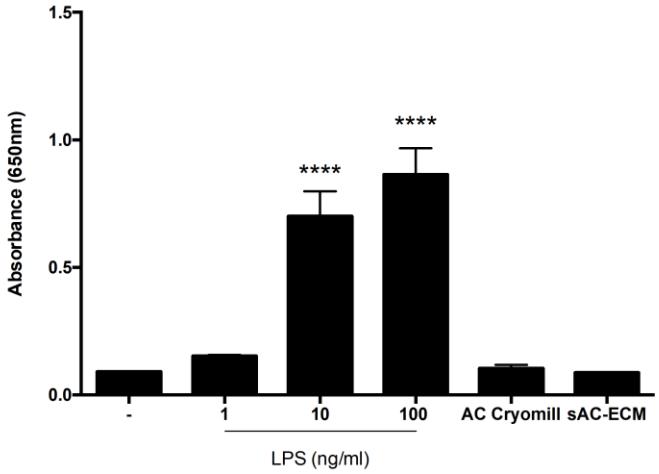

Supplementary Figure 1: Confirmation of Endotoxin free ECM Scaffolds. ECM scaffold preparations were shown to be endotoxin free, using the HEK-BlueTM hTLR4 assay system (Invivogen). The expression of SEAP, as measured by absorbance at 650nm, by scaffold treated macrophages was comparable to untreated control cells. As a positive control, cells were treated with LPS (1 ng/ml, 10 ng/ml or 100 ng/ml).

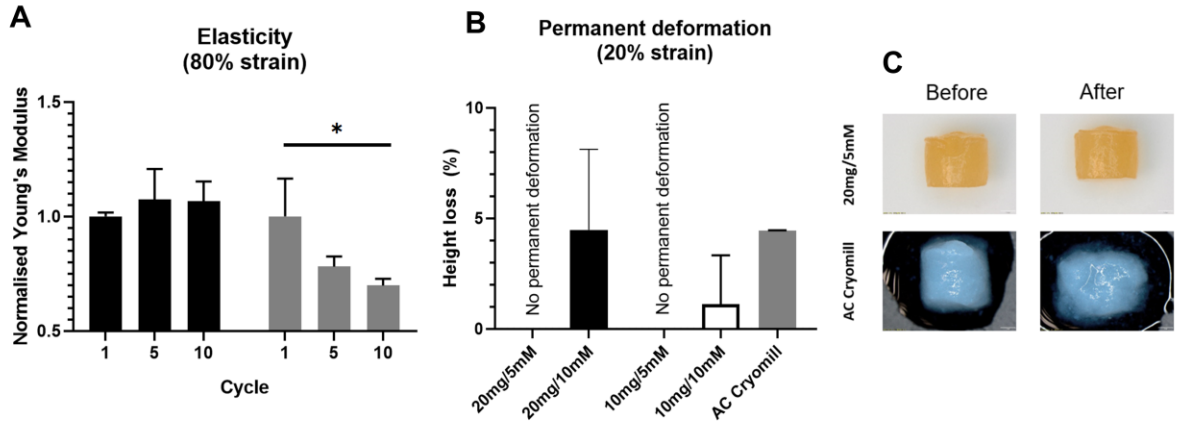

Supplementary Figure 2: Mechanical testing to demonstrate the different behaviour of solubilised ECM scaffolds and those produced using particulated ECM (AC-Cryomill). Cumulative percentage of the total height loss and height loss per cycle was calculated to characterize the super-elastic properties of the constructs. The percentage height loss of the scaffolds was determined at 20% strain (A). Scaffolds (Solubilized and AC-cryomilled) were subjected to 80% strain to determine elasticity (B&C).